

String-Like Collective Atomic Motion in the Melting and Freezing of Nanoparticles

Hao Zhang* and Pranav Kalvapalle

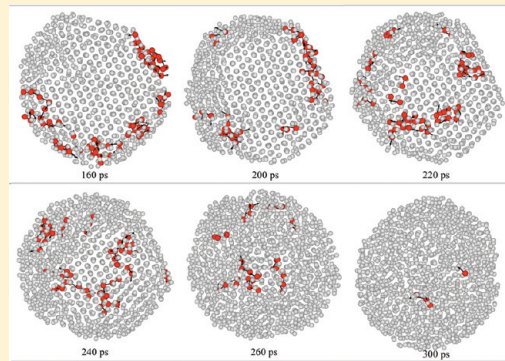
Department of Chemical and Materials Engineering, University of Alberta, Alberta, T6G 2 V4 Canada

Jack F. Douglas*

Polymers Division, NIST, Gaithersburg, Maryland 20899, United States

 Supporting Information

ABSTRACT: The melting of a solid represents a transition between a solid state in which atoms are localized about fixed average crystal lattice positions to a fluid state that is characterized by relative atomic disorder and particle mobility so that the atoms wander around the material as a whole, impelled by the random thermal impulses of surrounding atoms. Despite the fundamental nature and practical importance of this particle delocalization transition, there is still no fundamental theory of melting and instead one often relies on the semi-phenomenological Lindemann-Gilvarry criterion to estimate roughly the melting point as an instability of the crystal lattice. Even the earliest simulations of melting in hexagonally packed hard discs by Alder and Wainwright indicated the active role of nonlocal collective atomic motions in the melting process, and here we utilize molecular dynamics (MD) simulation to determine whether the collective particle motion observed in melting has a similar geometrical form as those in recent studies of nanoparticle (NP) interfacial dynamics and the molecular dynamics of metastable glass-forming liquids. We indeed find string-like collective atomic motion in NP melting that is remarkably similar in form to the collective interfacial motions in NPs at equilibrium and to the collective motions found in the molecular dynamics of glass-forming liquids. We also find that the spatial localization and extent of string-like motion in the course of NP melting and freezing evolves with time in distinct ways. Specifically, the collective atomic motion propagates from the NP surface and from within the NP in melting and freezing, respectively, and the average string length varies smoothly with time during melting. In contrast, the string-like cooperative motion peaks in an intermediate stage of the freezing process, reflecting a general asymmetry in the dynamics of NP superheating and supercooling.



INTRODUCTION

The theory of melting has developed rather slowly, and there is still no generally accepted theory of this ubiquitous phenomenon. Melting has often been conceived in terms of local defect formation such as the proliferation of vacancies upon heating¹ or the formation of interstitials^{2–4} and dislocations^{5–8} where these thermal “excitations” progressively decrease the shear modulus of the crystal lattice until there is a complete loss of rigidity, resulting in a fluid state. Chui^{9–11} has emphasized the importance of the self-organization of dislocations to form low-angle grain boundaries that arise from their long-ranged interactions, an effect that when prevalent can drive the melting transition to be first order in two dimensions.^{12,13} There is also the Lindemann-Gilvarry approach to melting,^{14–19} which is based on a consideration of the global instability of the crystal lattice. In this perspective, melting is associated with a dynamical instability defined by the thermodynamics of the crystal. In particular, melting is then characterized by a condition at which the mean square atomic displacements become sufficiently large in comparison with the mean

interatomic distance for the lattice. Basically, this condition defines the point at which the crystal lattice loses its structural integrity.

All of these models consider melting in terms of time-averaged equilibrium properties and focus on the derivation of the conditions under which melting occurs and the thermodynamic nature of the melting transition, that is, phase transition order.²⁰ These approaches generally neglect local dynamical phenomena involving the nonequilibrium progressive change of state of the material state from a locally ordered to a disordered state or the reverse of this process, “freezing”. Measurements of freezing provide ample evidence of large-scale fluctuations in dynamic light scattering measurements,²¹ an effect attributed to some kind of large-scale collective atomic motion at the crystallization front.²² In the present

Special Issue: H. Eugene Stanley Festschrift

Received: April 22, 2011

Revised: June 6, 2011

Published: June 30, 2011

work, we seek to better understand the character of the collective motion exhibited at melting and crystallization fronts under highly nonequilibrium conditions and the potential relation of this phenomenon to the collective motion observed in glass-forming (GF) liquids and the interfacial dynamics of nanoparticles (NPs) under equilibrium or quasi-equilibrium conditions.

The various proposed models of melting discussed before lead us to expect some kind of thermally activated “defects” to form during the course of phase transformation that self-organize into spatially extended coherent structures which “drive” the melting transition. In crystallization, ordered nuclei somehow self-organize from the disordered fluid, and these structures then progressively coarsen through a process that must involve cooperative atomic motion. We identify and examine the nature of these collective motions and supramolecular organization processes in melting and crystallization by molecular dynamics. For this purpose, we consider the melting of metal NPs because their melting temperature T_m can be tuned through their size, the system size is accessible for MD computations, and NP melting has its own interest.

We first quantify the melting temperature T_m of our simulated NPs and then examine the nature of the collective motion and average local particle displacement dynamics of the Ni atoms within the melting NP using the same numerical metrologies as in our previous complementary study of the dynamics of GB in polycrystalline Ni²³ and the interfacial dynamics of Ni NPs under equilibrium conditions.²⁴ We find the same type of collective atomic motion that we have found before to characterize the atomic motions of GB and the interfacial dynamics of Ni grains and NP, respectively. When the temperature is jumped to a value above the NP melting temperature, collective atomic motions leading particle disorganization initiate from the NP interface and propagate wave-like into the NP interior, resulting in the melting of the entire NP. We also observe the outward growth of crystal ordering from a seed within the NP core, where the interfacial layer separating the ordered and disordered regions of the material are characterized by highly cooperative atomic motions reminiscent of those found in the GB of polycrystalline materials. A large asymmetry in the propensity toward superheating the NP crystal and supercooling the NP liquid drop is observed because of the facile “nucleation” of melting by the collective interfacial motions normally present at the interface near the melting temperature and the relative difficulty in forming nuclei of ordered crystal within the NP. In the present work, we introduce crystal nuclei into the NP core to facilitate the initiation of crystallization.

SIMULATION DETAILS

Molecular dynamics simulations were performed to characterize melting/freezing, and the string-like collective atom motions of NPs associated with the dynamics of the melting/freezing process. The atomic interactions were described using the Voter-Chen²⁵ form of an embedded atom method (EAM)²⁶ potential for Ni. Free boundary conditions (free surfaces with vacuum) were applied in all simulations, which were performed within a canonical ensemble (NVT), where a constant temperature (T) was maintained using the Nosé-Hoover^{27,28} method. We focused on Ni NP having 2289 Ni, which corresponds to an NP having a diameter of ~4 nm. The Ni NPs were initiated from an approximately spherical shape and a perfect local face-centered cubic structure. To achieve equilibrium, we subsequently relaxed the NPs at room T for 1.5 ns with zero angular and linear momentum values.

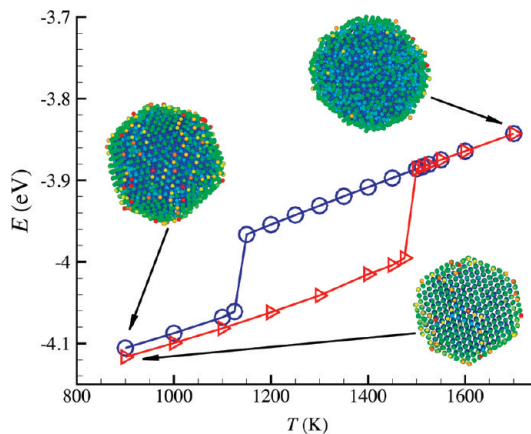


Figure 1. Potential energy per atom for heating and cooling cycles of a Ni cluster composed of 2899 Ni atoms.

Uncertainties below are based on a 95% confidence interval. The MD simulations utilize LAMMPS,²⁹ which was developed at the Sandia National Laboratories.

RESULTS AND DISCUSSION

As in the case of bulk materials, atomic mobility is largely controlled by the proximity of T to T_m . In the previous paper,²⁴ we estimated T_m of the NP by calculating the potential energy per atom (at each temperature, the potential energy is averaged over at least 300 ps) upon heating and then determining T_m as the T corresponds to the abrupt change in potential energy. The freezing temperature of the NP can be similarly determined by subjecting the NP to a cooling history in which T_f corresponds to the T where the potential energy drops abruptly.

Figure 1 shows the potential energy E versus T for both heating and cooling in the illustrative case of a Ni NP with 2899 atoms, corresponding to a NP with a diameter of ~4 nm. The heating and the cooling rate in current simulations are 1.0×10^{11} and 5.0×10^{10} K/s, respectively, where the potential energy is averaged over the last 300 ps of the final temperature. The heating and cooling curves in Figure 1 reveal a significant hysteresis effect in which the fluid state persists for a significant range below T_m . Whereas the fluid state exhibits metastable equilibrium behavior below T_m , the melting process does not exhibit superheating. Melting is evidently “easier” for the NP, and we next consider the nature of this process.

The NP surface atoms are less constrained in their motion (see quantification below) than the NP core atoms, and we then expect the surface atoms in the NP crystal to be more mobile than the core atoms. In our previous paper, we showed that the interfacial atomic motions of the NPs at thermodynamic equilibrium take the form of collective string-like motions that are exactly of the kind found in GB dynamics and the dynamics of GF liquids.²³ These transient string-like structures exhibit a universal exponential size distribution, and the average extent (length) of this string-like cooperative motion grows upon cooling, in parallel to the growth of the activation energy for atomic transport.²⁴ Previously, we also introduced a method for determining how the average string length evolves in length, following a jump from one temperature to another, allowing us to follow the physical aging of the NP dynamics. We next extend this methodology to a description to the nonequilibrium situation

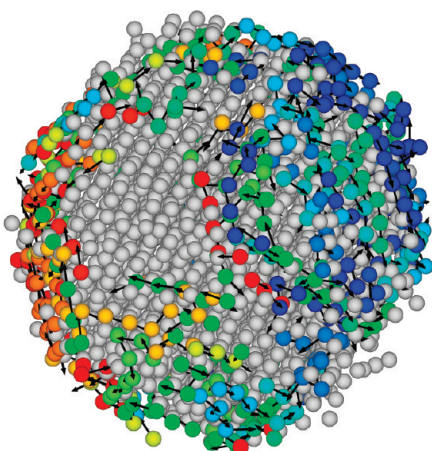


Figure 2. String-like collective atomic motion on the surface of a Ni nanoparticle at equilibrium. The lines denote Ni atoms that belong to the same collective atom movement and the colors are discriminate between distinct strings where $T = 1450$ K; $N = 2899$ corresponds to a NP having a radius equal 2 nm.

in which the initial state is a crystal at equilibrium at $T = 1450$ K, below the NP melting temperature T_m of 1500 K, and the T is then jumped to 1500 K, which results in the melting of the NP. (See Figure 1.) The first question that we investigate is how the string-like collective motion evolves during the melting process.

Cooperative Atomic Motion in NP Interfacial Dynamics and NP Melting. Cooperative particle dynamics is one of the most characteristic features of the dynamics of GF fluids. Both atomistic simulations^{30–32} and experiments³³ on GF colloidal³⁴ and granular fluids³³ exhibit strings and MD simulations^{23,35,36} have recently shown that this type of motion also occurs in the dynamics of GB. We next apply methods originally developed to identify this type of correlated motion in GF liquids³⁰ to our simulations of the dynamics NP melting. First, we review the collective atomic motion that occurs on the NP surface at equilibrium as a reference point below.

As a first step in identifying collective particle motion, we must identify the “mobile” atoms in our system. In GF liquids, the mobile atoms (atoms with enhanced mobility relative to Brownian motion) are defined by comparing the self-part of the van Hove correlation function $G_s(r)$, describing the probability distribution that a particle initially at the origin makes a displacement to the spatial distance $r(t)$ after a time t for the strongly interacting particle fluid to an ideal uncorrelated liquid exhibiting Brownian motion where $G_s(r)$ reduces to a simple Gaussian function by the central limit theorem. (The diffusion coefficient D is defined to be the same in the interacting and noninteracting $G_s(r)$).³⁰ The interacting fluid $G_s(r)$ has a long tail at large distances, r , pointing to the existence of particles of relatively high mobility in the interacting particle system. A comparison of this kind is generally made to a crossing of the interacting and noninteracting $G_s(r)$ curves, and the mobile particles are then naturally defined as those atoms whose displacement exceeds the crossing point distance after a characteristic diffusive decorrelation time Δt defined by the fourth and second moments of $G_s(r)$.³⁰ Because mobile atoms are essentially those particles moving a distance $r(t)$ larger than the typical amplitude of an atomic vibration after a decorrelation time, Δt , but smaller than the second nearest-neighbor atomic distance, we mathematically identify these mobile particles, as in previous studies of GB dynamics and the interfacial dynamics of

NP^{23,24} by a threshold atomic displacement condition, $0.35r_0 < |\mathbf{r}_i(\Delta t) - \mathbf{r}_i(0)| < 1.2r_0$, involving the bulk interatomic spacing, r_0 .

The identification of correlated atom motion requires a consideration of the relative displacement of particles. Collective atomic motion means that the spatial relation between the atoms is preserved to some degree as the atoms move. Specifically, reference mobile atoms i and j are considered to be within a collective atom displacement string if they remain in each other's neighborhood, and we specify this proximity relationship by, $\min[|\mathbf{r}_i(\Delta t) - \mathbf{r}_j(0)|, |\mathbf{r}_j(0) - \mathbf{r}_i(\Delta t)|] < 0.43r_0$, as in past studies of GF liquids, the dynamics of GB^{30,35} and the interfacial dynamics of Ni NP.²⁴ Application of this criterion reveals that the collective particle motion in the NP interfacial region takes the form of “strings”. (See Figure 2 for illustration.) The nature of this motion is remarkably similar to previous simulations on the atomic dynamics of GF liquids³⁰ and the atomic dynamics GB in polycrystalline materials.^{23,37}

The mean “string length”

$$\bar{n}(\Delta t) = \sum_{n=2}^{\infty} n P(n, \Delta t) \quad (1)$$

provides a measure of the scale of cooperative particle motion in strongly interacting liquids, where $P(n, \Delta t)$ is the probability of finding a string of length n in time interval Δt . String properties are defined at a characteristic decorrelation time $\Delta t = t^*$, at which the mean string length in eq 1 has a maximum.^{30–32,36} Previous work^{32,36} has established that the average string length in GF liquids grows upon cooling, along with the effective activation energy for structural relaxation. This finding accords with the Adam and Gibbs (AG) theory of relaxation in GF liquids,³⁸ where the strings are identified³⁰ with the vaguely defined “cooperatively rearranging regions” of the AG theory. Strings are thus of practical interest because they are correlated with the relative strength of the T -dependence of transport properties (see below), perhaps the most important property of GF fluids.

String-like cooperative atomic motion is prevalent in all GF liquids examined to date (including water, polymer fluids, metallic glass-forming liquids, concentrated colloidal suspensions, and even strongly driven granular fluids.^{30,32,34,37,39}) It is apparently a universal property of the dynamics of strongly interacting fluids where a strong reduction in the particle mobility and an enormous change in the rate of structural relaxation are found in association with the growth of string-like correlated motion upon approaching the glass-transition temperature, T_g . We next examine the nature of the atomic motion occurring on the NP surface to determine if it follows this general pattern of “frustrated fluid” dynamics. Figure 2 shows typical particle displacement strings in our simulation appearing on the outer skin of our simulated Ni NP at $T = 1450$ K. The colored atoms represent the initial atomic positions ($t = 0$), and the displacement arrows point to their positions at a later time Δt . This string-like atomic motion occurs predominately on the surface of the NPs, and we discuss this atomic motion in relation to our previous paper on NP interfacial dynamics.²⁴

Atomistic simulations of glass-forming liquids indicate that the distribution of string lengths $P(n)$ is generally an exponential function of n ,

$$P(n) \approx \exp(-n/\langle n \rangle) \quad (2)$$

to an excellent approximation. Figure 3 of ref 24 shows the distribution of string lengths at $\Delta t = t^*$, where the mean string

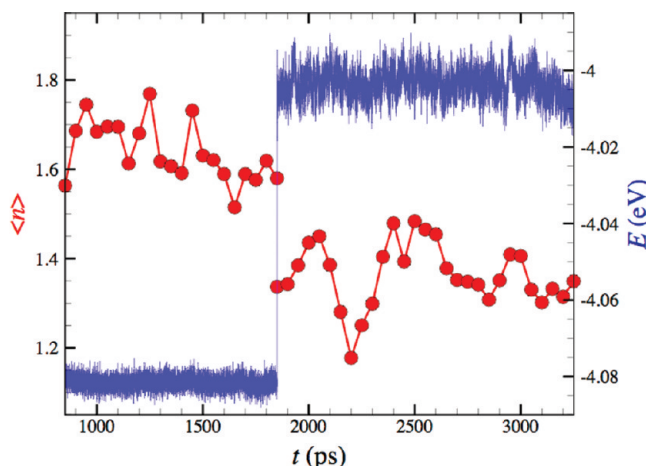


Figure 3. Evolution of the average string length $\langle n \rangle$ characterizing the interfacial atomic motions of a NP ($N = 2899$, corresponding to NP radius = 2 nm) following an upward jump of the T to a new steady value below the T_m of the NP.

length $\bar{n}(\Delta t)$ exhibits a maximum [time dependence of $\bar{n}(\Delta t)$ not shown (see refs 30, 31, 36)]. Interestingly, the distributions of n in the interfacial region of the Ni NPs are essentially the same as those found both in GF liquids⁴⁰ and in the atomic dynamics of GB in simulated polycrystalline Ni.²³ Moreover, the magnitude of $\langle n \rangle$ is comparable to values found in GF liquids and GB when compared in the same range of reduced T range. In the Supporting Information, we summarize information on the Debye–Waller factor of the NP interfacial atoms and those on the NP interior that is useful in characterizing the characteristic temperatures governing the glassy interfacial dynamics of the NP under equilibrium conditions.²⁴ This data is a natural point of reference in our discussion below.

We may infer from the previous discussion that string-like atomic motion occurs under more general circumstances than glass formation. This phenomenon effect was also observed long ago as a conspicuous feature of MD simulations of melting in bulk materials,⁴¹ but these studies sought no quantification of the effect, as we have discussed above for the NP interfacial dynamics. We next consider nonequilibrium phenomena associated where string dynamics evolves over time.

Previous studies of the collective dynamics of GF fluids and the dynamics of GBs were restricted to constant temperature and equilibrium conditions. The existence of long relaxation times in GF liquids, associated with necessity of collective atomic motions, means that sample equilibration can be extremely slow in these systems and that there should be a slow evolution of the average string size to larger values after the T is lowered or corresponding shrinking of the average string length in time if the system is heated (provided T is well below T_m of the NP; see Figure 3).

To calculate the time dependence of the average string length, we simply determine $\langle n \rangle$ using eq 2 through the string distribution function with respect to time points t displaced at fixed times with respect to an initial reference time where a temperature jump is made from some initial T_i to some final lower temperature T_f ; all temperatures are below T_m so that strings having a nontrivial average length exist. Figure 3 shows the resulting evolution in the average string length resulting from a temperature jump where $T_i = 1100$ K and $T_f = 1450$ K. As expected, we observe a progressive evolution of the string length to a lower value upon raising T . In the

equilibrium state, the average string length exhibits fluctuations about the average value, the amplitude of which depends on T , just as in particle systems that self-assemble into strings.^{42,43} This phenomenon is natural because string formation in glass formation is consistent with this process being a kind of self-assembly.³⁹ This observation opens up the possibility of a more quantitative analysis of the relaxation dynamics of glass-forming liquids⁴⁴ and string formation in other contexts, such as the present example of NP interfacial dynamics. Moreover, the calculation of the dynamics of string formation and disintegration when the material is perturbed by changes in temperature, stress, illumination, and so on and recent developments in the modeling the fundamental thermodynamics and dynamics of particle string formation in associative particle systems^{45,46} provides a methodology for exploring a host of interesting nonequilibrium condensed matter phenomena: the dynamics of melting, freezing, nucleation, particle sintering, 1/f noise in transport, and so on.

String Dynamics Accompanying NP Melting and Freezing.

Our new paradigm for understanding interfacial NP dynamics emphasizes the importance of string-like collective atom motion in understanding the transport properties of these particles in a unified way with polycrystalline materials, GF liquids, and even other strongly interacting fluids such as granular fluids³⁷ and plasmas.⁴⁷ We now apply this perspective to gain insight into NP melting and freezing.

We first emphasize that the appearance of string-like collective motion in connection with melting has been apparent from simulations of hard disk melting by Alder and Wainwright^{48,49} and the melting of 2D Lennard-Jones particle lattices.⁵⁰ This particle permutation motion has also been observed in particle tracking measurements of melting in quasi-2D lattices of colloidal particles,^{51–54} quasi-2D driven granular fluids,⁵⁵ and simulations of the melting of quasi-2D plasma crystals.^{11,56,57} It is thus not surprising that we see prevalent string-like collective motion in our simulations of NP melting.

Next, we consider a temperature jump from the equilibrium situation shown in Figure 2, where $T = 1450$ K, and follow the evolution of the system after rapidly jumping the T to the NP melting temperature, $T = 1500$ K. The strings, located initially at the interface of the NP, follow a front of disordering that progressively invades the interior of the NP until the entire NP has melted. (See Figure 4.) The string-like motion of the NP at equilibrium apparently serves to initiate (“nucleate”) and to sustain the melting process at the propagating melt interface. Surface-induced melting initiating from the surface melted state below T_m has been directly observed in measurements on bulk materials, so this is certainly not a phenomenon limited to NP.⁵⁸ We next quantitatively examine the evolution in the string dynamics during the course of the NP melting using the method described above.

Figure 5 shows the evolution of the average string length and the average potential energy upon melting where the T -history is the same as Figure 4. The potential energy evidently rises in two stages during the melting process, and there are corresponding changes in the average string length demarking these melting regimes. We see that the amplitude of the string length fluctuations is relatively large in the first regime and the fluctuations in the string length and potential energy then stabilize after some initial collective particle rearrangements in this metastable state. After a relatively long period, the potential energy per atom smoothly increases from -3.96 to -3.88 eV as the NP evolves toward its fully melted equilibrium state at $T = 1500$ K. Before this final

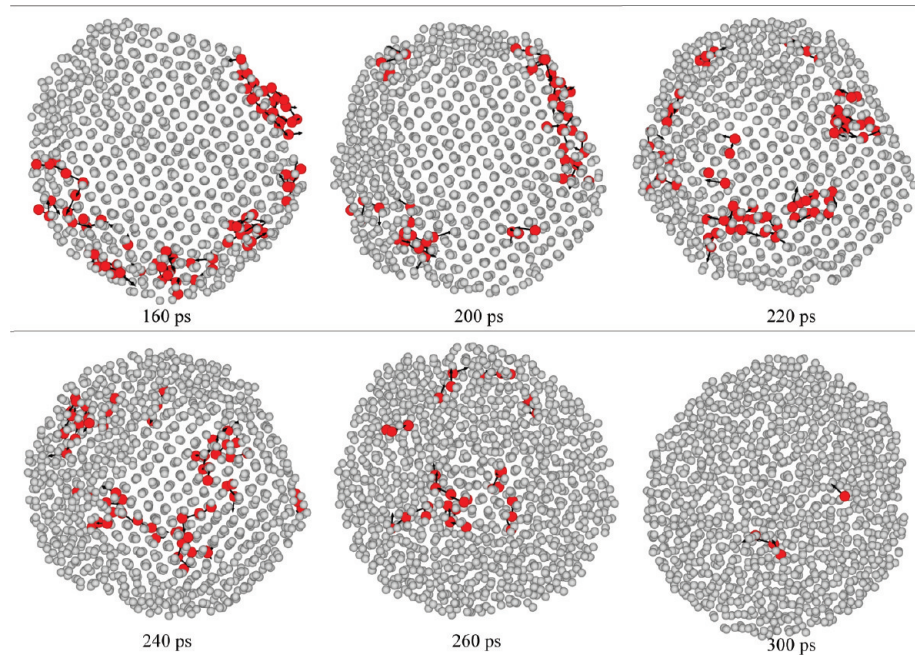


Figure 4. Series of atomic configurations showing the process of melting for the $N = 2899$ NP when the temperature is raised from 1450 to 1500 K and held at 1500 K afterward. For the sake of clarity, this view includes only those atoms in a 1 nm slab in the center of the NP. The red spheres represent the atoms at initial time t_0 , and the vectors point to the final time $t_0 + t^*$.

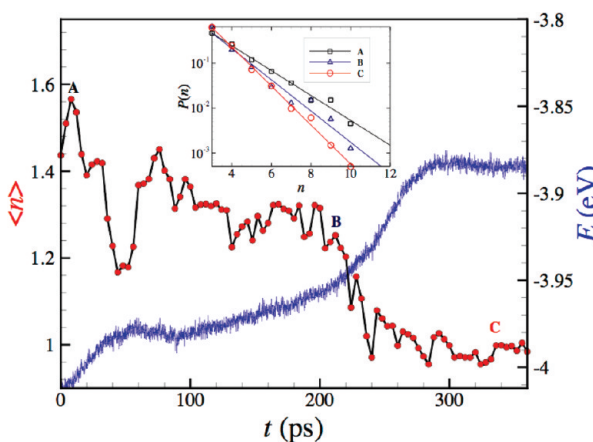


Figure 5. Evolution of the average string length $\langle n \rangle$ characterizing the interfacial atomic motions of an $N = 2899$ NP at $T = 1500$ K. The inset shows the size distribution of the collective atom motions at the representative time points A, B, and C in the main plot.

stage of NP melting ($100 \text{ ps} < t < 200 \text{ ps}$), the string length $\langle n \rangle$ exhibits significant fluctuations about an average value of ~ 1.3 and then drops sharply from this quasi-equilibrium value to ~ 1.0 , characteristic of the absence of collective atomic motion. The size distribution of the strings remains exponential throughout the nonequilibrium aging process, and we illustrate this distribution in the inset of Figure 5 for representative times (A, B, C) at the beginning, middle, and end of the melting process. The size distribution of dynamic particle chains of self-assembling (difunctional) patchy particles also evolves in a way in which the exponential length distribution is preserved as the polymer chains grow to their new equilibrium size following a T -jump to a lower temperature.⁴⁵ In each case, aging of the system can be given a direct

geometrical interpretation in terms of growing strings having a length distribution whose form is exponential and invariant in time.

We next consider the reverse nonequilibrium process of freezing. In particular, we reduce T from above the melting temperature ($T = 1500$ K) and follow the evolution of the system after cooling rapidly below the NP freezing temperature to $T = 1250$ K. (Because we have placed a crystal nuclei in the center of the NP, the freezing temperature increases in comparison with the NP without crystal nuclei; see Figure 1 where the potential energy per atom after freezing is higher than that of the NP without heating and cooling treatment). Again, we find strings preferentially located at the crystal–liquid boundary, and these structures grow outward from the NP core as the NP freezes, as shown in Figure 6. Wang et al.⁵⁹ have recently characterized this type of collective motion and evolving dynamic heterogeneity in the crystallization of Ni specified by an EAM potential (periodic boundary conditions because the calculations were intended to model a bulk material and $N = 4000$) and found qualitatively similar results.

The evolution in the strings during the course of NP melting is rather different from NP freezing. Figure 7 shows the evolution of the average string length for an equilibrium NP at $T = 1500$ K quickly quenched to $T = 1250$ K. Although the temperature $T = 1250$ K is well below the NP freezing temperature, crystallization does not occur immediately. Instead, the liquid phase remains in a metastable condition for a relatively long time where the potential energy per atom remains almost constant and where the average string length fluctuates only slightly from the average value, $\langle n \rangle = 1.06$. Evidently, the cooperative motions within the NP are weak in this metastable state. Crystallization is signaled by an abrupt drop in the potential energy from -3.94 to -4.04 eV. During this transformation, the average string length increases sharply, reaching a value near 1.7, which is close to the average value of the string length in glass-forming liquids near the temperature

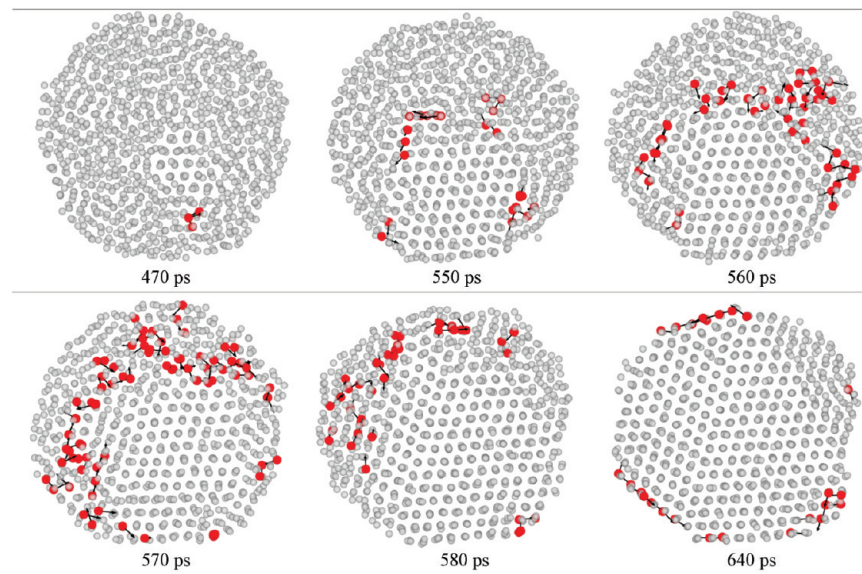


Figure 6. Series of atomic configurations showing the process of crystallization for the $N = 2899$ NP when the temperature is quenched to 1250 K. For the sake of clarity, this view includes only those atoms in a 1 nm slab in the center of the NP. The red spheres represent the atoms at initial time t_0 , and the vectors point to the final time $t_0 + t^*$.

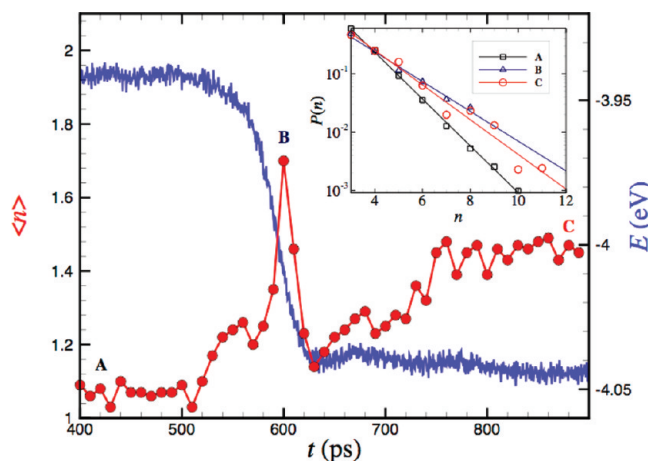


Figure 7. Evolution of the average string length $\langle n \rangle$ characterizing the interfacial atomic motions of an $N = 2899$ NP following a downward jump of the T to a new steady value. The inset shows the size distribution of the collective atom motions at the representative points A, B, and C in the main plot.

T_c , defining the onset of deep supercooling. This value of $\langle n \rangle$ is well above its equilibrium value $\langle n \rangle \approx 1.4$ at this temperature. Highly cooperative string-like motion is evidently a conspicuous aspect of particle motion during the freezing process. After cessation of the crystallization process, the average string length $\langle n \rangle$ returns to fluctuating about its average value, which for this T is ~ 1.42 .

Our simulation of the NP melting process suggests that the strings located initially at the surface of the NP tend to nucleate to form disordered regions that progressively invade the interior of the NP until the entire particle has melted. Therefore, it is natural to expect that any factor influencing the mobility of the interfacial atoms, will substantially affect properties relating to NP melting, e.g., the NP melting point, NP rigidity, and so on.

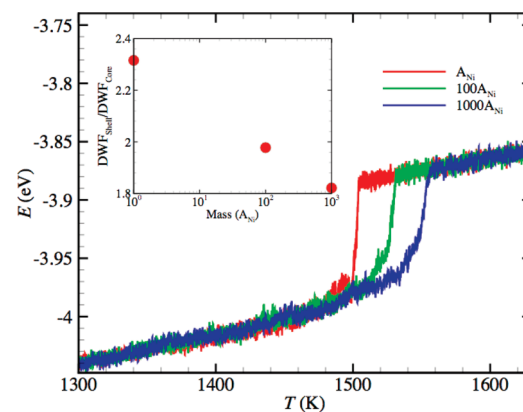


Figure 8. Potential energy per atom for heating of a Ni cluster composed of 2899 Ni atoms with outer shell atom having atomic mass that is 1, 100, and 1000 times the Ni atomic mass. Note that this modification of the interfacial atomic motion leads to a shift of T_m by ~ 50 K. The inset shows the ratio of Debye–Waller factor of the shell atoms to that of the interior atoms as a function of atomic weight of the shell atoms at $T = 600$ K.

To confirm this expectation, we consider an idealized system in which the atoms in the interfacial region of the NP are substituted by atoms with different atomic mass, but which have otherwise identical size and interatomic interactions. To highlight this effect, we formally change the mass of the atoms within a thickness of 3.5 Å skin of outer shell of the NP to 100 and 1000 times the Ni atomic mass. The large mass of the surface shell atoms will reduce the amplitude of atomic motion at a given T , and we can expect based on the foregoing qualitative reasoning to see a large increase in the melting temperature. Figure 8 shows the potential energy per atom for heating of a Ni cluster composed of 2899 Ni atoms with outer shell atoms having atomic mass of 1, 100, and 1000 times of nickel atom mass, where the continuous heating rate is again set at 1.0×10^{11} K/s.

Evidently, increasing atomic mass of outer shell atoms gives rise to a progressive rise in the NP melting temperature, as expected. The inset exhibits the ratio of Debye–Waller factor (see details in the Supporting Information) of the shell atoms to that of the interior atoms as a function of atomic mass of the shell atoms at $T = 600$ K. A modest change of $\langle u^2 \rangle$ evidently corresponds to a large T_m shift of ~ 50 K. This exercise illustrates how alteration of the dynamics of surface atoms can affect the NP melting point of NP, which in practice can be achieved in a myriad of ways such as alloying the NP with other metals, surface oxidation, the addition of organic capping layers such as self-assembled monolayers, grafted polymers such as DNA or polyethylene glycol, the adsorption of polymers such as proteins, or varying the medium in which the NP are placed, and so on. Large changes in the NP are generally expected from interfacial modification.

CONCLUSIONS

We use MD simulation to confirm our hypothesis that string-like cooperative motion plays an active role during NP melting and freezing. Moreover, we find that the atomic dynamics within the interfacial region of our Ni NPs under the conditions of melting and freezing exhibits many features in common with glass-forming liquids, the atomic dynamics of grain boundaries, and NP interfacial dynamics under equilibrium conditions. String-like collective motion is evidently a basic phenomenon in condensed matter systems and fluctuations in various ordering processes are expressed through this ubiquitous low-energy type of collective density fluctuation.

The reason for the general occurrence of string-like collective particle motion in diverse near-equilibrium, but strongly interacting, equilibrium or near-equilibrium particle systems such as glass-forming liquids, the grain boundaries of polycrystalline materials, and the interfacial dynamics of NPs, and its occurrence also in highly nonequilibrium materials exhibiting both melting and freezing transitions is difficult to explain because melting, crystallization, and glass-formation all lack fundamental theoretical descriptions. Nonetheless, all of these material systems have physical features in common that probably underlie the generality of this phenomenon. In each of these systems, there are either competing packing states in “frustrated” particles cannot participate in some state of relatively high packing efficiency or in which some particles are orientationally frustrated because they cannot simultaneously conform to the competing constraints of ordered domains having distinct orientations, as found in polycrystalline materials. In glass-forming liquids, the particles locally pack in a way that is more efficient than any macroscopic equilibrium crystal of the material, such as local icosahedral packing in spherical particle systems found in hard sphere colloidal and metallic glass-forming liquids, and the string-like collective motion then occurs in less “well-packed” (the local density changes can be extremely small so that free volume or local density variations then do not allow for the prediction of local mobility variations) fluid regions. At equilibrium, the relatively immobile well-packed particle domains exchange dynamically at equilibrium with the mobile frustrated particles exhibiting string motion. In NPs, the physical situation is somewhat similar physically to grain boundaries and glass-forming liquids; the ordered atoms in the particle core are separated by the NP exterior region, which is normally either a completely disordered fluid or in a gas state populated by a different type of molecule. The interfacial atoms of the NP are in this case frustrated between adopting the extremely different

ordering states of their interior and exterior environments. Now in NP freezing and melting, respectively, a crystal nucleus normally grows from within the particle or the particle “melts” through nucleation from its surface. In each case, an interface that separates regions of relative order and disorder in the NP must propagate so that there are inevitably frustrated atoms in the interfacial region of these ordering and disordering fronts. The particle dynamics within both melting and crystallization fronts can then be naturally expected to exhibit a dynamics similar to strongly interacting fluids at equilibrium because of a similar frustration in packing. Of course, this does not explain such striking features as the tendency of the length distribution of the strings to remain exponential under strongly nonequilibrium conditions, as we observe. Perhaps our observations simply imply the existence of some local equilibrium in the developing ordering and disordering fronts?

We also anticipate, based on our previous experience with glasses, NPs and grain boundaries, that melting in macrocrystalline materials should also be largely dominated by string-like collective motion because this process is now thought to be characterized by the spontaneous formation of thermally excited grain boundaries^{9–11} and because particle motion in such mobile grain boundaries tends to be dominated by string-like particle displacements. Indeed, the very sharpness of the melting transition of solids, recognized technically in terms of the first-order nature of this transition in bulk materials and from everyday experience, might then be a direct consequence of highly cooperative string molecular motion that allows the grain boundaries to free slide with little frictional resistance so that the material sharply loses its “cohesiveness”. The role of string motion in the melting of bulk crystals and of polycrystalline materials having impurities is an obvious topic for future simulation studies.

These simple observations about the origin of collective atomic motion in diverse strongly interacting particle systems, both under equilibrium and far from equilibrium conditions, point to the practical significance of this phenomenon in numerous further contexts of fundamental scientific and practical interest in material science and biology. For example, can we describe the conspicuous physical aging of glasses, the evolution of the structural relaxation time, and other glass properties over time at low temperatures,⁶⁰ in terms of the evolution of the string length in time? Recently, changes in the string length have been shown to predict quantitatively changes of the relaxation time with temperature in polymer nanocomposites,⁶¹ when the strings are identified with the cooperatively regions of Adam and Gibbs.⁶² Can we simply replace the time dependence of the string length $L(t)$ in glass-forming liquids, as determined in the present work, by the equilibrium value of L as in Starr and Douglas⁶¹ to predict fully the evolution of the structural relaxation time τ in aging glassy materials? Alternatively, can we describe “rejuvenation” phenomena glass-forming liquids following application of stress^{63,64} in a way similar to mechanically disturbed complex fluids exhibiting supermolecular assembly where the return to equilibrium is understood in terms of the regrowth of the string-like equilibrium polymer excitations³⁹ in the nonequilibrium glass-forming liquid. Confirmation of this physical picture of aging would open many opportunities for modeling physical aging because there are now validated analytic models of the equilibrium polymerization under both equilibrium and nonequilibrium growth conditions.^{65–67} Furthermore, can we then study the evolving plasticity of deformed materials in terms of a string evolution with t and the extent, rate, and type of mechanically deformation of the material (e.g., compression versus extension)? Investigation of the plasticity of amorphous and

semicrystalline materials from the standpoint of string dynamics promises to be a rich field of study.

Collective particle dynamics is also probably a basic characteristic of soft biological materials broadly, and the implications of string-like collective motion in biology are probably diverse and deeply significant with respect to disease, medical treatment, and to a basic understanding of biological materials. Recently, cell displacement dynamics strikingly similar to glass-forming liquids has been observed when they are moving and proliferating in model tissues created *in vitro*.⁶⁸ It is then a next natural step to examine whether string-like collective motions are also characteristic of cell motion in biofilms, animal tissue, and other collective states of “higher” biological organization (e.g., brain tissue) and whether such motions, if observed, are important for essential biological activities. On a finer scale, proteins have been described as being akin to “surface-melted solid particles”,⁶⁹ so it is also natural to consider whether the molecular motions within proteins exhibit the same type of universal string-like collective motions on an atomic scale as we have found in the interfaces of inorganic NPs.²⁴ In other words, can we reasonably adopt the paradigm that proteins are just “organic NPs” whose powerful catalytic properties have a common origin with inorganic NPs by virtue of their capacity for a similar type of collective atomic motion? This basic question can be readily investigated by molecular dynamics simulation, and if this type of collective motion is indeed common to these systems, as we expect, then far reaching ramifications for our understanding of both enzyme and inorganic catalytic behavior might follow. We also note that the lipid membranes of living cells are complex lipid mixtures that are permeated by proteins and other molecules that inhibit lipid crystallization; it certainly seems reasonable to describe such complex materials as glass-forming liquids and to investigate fluidity changes in these systems in terms of agents and environmental perturbations that alter the collective molecular motion within these complex fluids. In our view, this perspective of lipid membranes offers the potential for a paradigm shift in our understanding of the membranes and in our understanding and approach to numerous diseases and medical effects associated with drugs, toxins, protein aggregation processes that disrupt proper membrane function in living cells, and thus organism health through their influence on the membrane molecular packing efficiency and the membrane fluidity.

Evidently, because string-like collective motion in condensed matter systems seems to be broadly associated with “packing frustration”, essentially any type of perturbation (e.g., hydrostatic pressure, molecular and NP additives, nanoconfinement, alloying, flow, the presence of solvents on the interfacial dynamics, finite size variation such a particle size, feature size, or film thickness or feature size in materials of nanometer dimensions, or even illumination when transitions in electronic states and changes of molecular conformation arise) influencing packing efficiency could significantly alter the properties of “soft” materials. This seems to offer numerous strategies to modulate collective string dynamics in soft materials to tailor their properties. In particular, the susceptibility of these complex materials to perturbation provides many opportunities for design of new functional materials and for understanding the high biological activity of NPs and other nanostructured materials. Of course, there are also measurement challenges in quantifying these property changes. Aging associated with slow string evolution can be expected to be particularly troubling in materials fabrication and measurement contexts because material properties can be expected to drift slowly and

significantly over time because the slow attainment of equilibrium is intrinsic to “glassy” systems. Changes in the local chemical and physical environment of these particles further convolute effective characterization of these materials because these factors must also generally alter the string evolution.

Regarding NPs in particular, the highly cooperative string-like atomic motion in the interfacial region of NPs makes them particularly susceptible to property changes associated with the natural variables of particle size and surface functionalization to disperse and stabilize them. An understanding of this interfacial dynamics can be expected to shed significant light on changes in the mechanical properties of these particles with particle size and through coating and functionalization, the process of sintering,^{70,71} melting,⁴¹ and crystal nucleation.⁵⁹ Our viewpoint of NPs as generally having a highly dynamic interfacial dynamics, as in the case of proteins, is contrasted with the more conventional static picture of these structures that emphasizes idealized zero temperature particle condition where the particle is imagined in terms of static faceted crystals, albeit corrugated by the atomic nature of the crystal lattice. Real NPs at finite temperatures can be remarkably dynamic. Moreover, the coupling of the cooperative interfacial dynamics of NPs and other materials exhibiting this type of interfacial collective motion (possibly including proteins and lipid membranes from the discussion above as well a manufactured nanostructures) with the cooperative motions within the solvent in which the particles are placed promises to be a very rich field of study. Water itself exhibits collective string-like molecular motion even at room temperature,⁷² and these collective motions can be expected to modify those of the NP, perhaps even driving these interfacial motions so that the motions of the particle become enslaved to those of the solvent in cases where the interfacial motion is highly active because of its small size or interfacial modification through molecular adsorption, hydration, metallic alloying, chemical change, or the grafting of polymer chains to the surface to aid NP dispersal.

Our unified description of the dynamics of grain boundaries, NP interfacial dynamics, and glass-forming liquids can be immediately useful in the design of new materials by “translating” results, or at least questions, from one field of study to another. For example, recent MD simulations⁷³ have considered the effect of “dopant” atom size interaction on the molecular dynamics of grain boundaries, and we can try to immediately test insights gained from this type of study to the interfacial dynamics of NPs. This analogy should also work in the reverse direction, and simulation results and empirical results from glass-forming liquids can be naturally compared with the interfacial dynamics of NPs, and a comparison of this kind shows striking parallels.^{24,60} This new perspective of the origin of the special and tunable properties of NPs offers the promise of an improved rational control of NPs properties, catalytic behavior, and improved particle stability based on further quantification and manipulation of their interfacial chemistry and physical environment.

■ ASSOCIATED CONTENT

S Supporting Information. Characteristic temperatures of NP and other aspects of the phenomenology of GF liquids that have significance for understanding the NP interfacial dynamics. Average mean square particle displacement of interfacial and crystal core atoms of a Ni nanoparticle relative to the square of the average interparticle distance. This material is available free of charge via the Internet at <http://pubs.acs.org>.

■ AUTHOR INFORMATION

Corresponding Author

*E-mail: hao.zhang@ualberta.ca (H.Z.). jack.douglas@nist.gov (J.D.).

■ ACKNOWLEDGMENT

H.Z. and P.K. gratefully acknowledge the support of the Natural Sciences and Engineering Research Council of Canada through the Discovery Grant program. J.F.D. acknowledges support of this work under the NIH grant (1 R01 EB006398-01A1).

■ REFERENCES

- (1) Frenkel, I. A. I. *Kinetic Theory of Liquids*; Dover Publications: New York, 1955.
- (2) Lennard-Jones, J. E.; Devonshire, A. F. *Proc. R. Soc. London, Ser. A* **1939**, *170*, 464.
- (3) Granato, A. V. *Phys. Rev. Lett.* **1992**, *68*, 974.
- (4) Kanigel, A.; Adler, J.; Polturak, E. *Int. J. Mod. Phys. C* **2001**, *12*, 727.
- (5) Kuhlmann, D. *Phys. Rev.* **1965**, *140*, 1599.
- (6) Kosterlitz, J. M.; Thouless, D. J. *J. Phys. C: Solid State Phys.* **1973**, *6*, 1181.
- (7) Cotterill, R. M. J. *Phys. Rev. Lett.* **1979**, *42*, 1541.
- (8) Edwards, S. F.; Warner, M. *Philos. Mag. A* **1979**, *40*, 257.
- (9) Chui, S. T. *Phys. Rev. B* **1983**, *28*, 178.
- (10) Mott, N. F.; Gurney, R. W. *Trans. Faraday Soc.* **1939**, *35*, 0364.
- (11) Quinn, R. A.; Goree, J. *Phys. Rev. E* **2001**, *6405*, 051404.
- (12) Janke, W.; Kleinert, H. *Phys. Rev. B* **1990**, *41*, 6848.
- (13) Kleinert, H. *Gauge Fields in Condensed Matter*; World Scientific: Teaneck, NJ, 1989.
- (14) Lindemann, F. A. *Phys. Z.* **1910**, *11*, 609.
- (15) Gilvarry, J. J. *Phys. Rev.* **1956**, *102*, 308.
- (16) Bilgram, J. H. *Phys. Rep.* **1987**, *153*, 1.
- (17) Lowen, H. *Phys. Rep.* **1994**, *237*, 249.
- (18) Finken, R.; Schmidt, M.; Lowen, H. *Phys. Rev. E* **2002**, *65*, 016108.
- (19) Luo, S. N.; Strachan, A.; Swift, D. C. *J. Chem. Phys.* **2005**, *122*, 194709.
- (20) Ramakrishnan, T. V.; Yussouff, M. *Phys. Rev. B* **1979**, *19*, 2775.
- (21) Dinardo, S.; Bilgram, J. H. *Phys. Rev. B* **1995**, *51*, 8012.
- (22) Burke, E.; Broughton, J. Q.; Gilmer, G. H. *J. Chem. Phys.* **1988**, *89*, 1030.
- (23) Zhang, H.; Srolovitz, D. J.; Douglas, J. F.; Warren, J. A. *Proc. Natl. Acad. Sci. U.S.A.* **2009**, *106*, 7735.
- (24) Zhang, H.; Kalvapalle, P.; Douglas, J. F. *Soft Mater.* **2010**, *6*, 5944.
- (25) Voter, A. F.; Chen, S. P. *Mater. Res. Soc. Symp. Proc.* **1987**, *82*, 175.
- (26) Foiles, S. M.; Baskes, M. I.; Daw, M. S. *Phys. Rev. B* **1986**, *33*, 7983.
- (27) Nose, S. *J. Chem. Phys.* **1984**, *81*, 511.
- (28) Hoover, W. G. *Phys. Rev. A* **1985**, *31*, 1695.
- (29) Plimpton, S. *J. Comput. Phys.* **1995**, *117*, 1.
- (30) Donati, C.; Douglas, J. F.; Kob, W.; Plimpton, S. J.; Poole, P. H.; Glotzer, S. C. *Phys. Rev. Lett.* **1998**, *80*, 2338.
- (31) Donati, C.; Glotzer, S. C.; Poole, P. H.; Kob, W.; Plimpton, S. J. *Phys. Rev. E* **1999**, *60*, 3107.
- (32) Riggleman, R. A.; Yoshimoto, K.; Douglas, J. F.; de Pablo, J. J. *Phys. Rev. Lett.* **2006**, *97*, 045502.
- (33) Marcus, A. H.; Schofield, J.; Rice, S. A. *Phys. Rev. E* **1999**, *60*, 5725.
- (34) Weeks, E. R.; Crocker, J. C.; Levitt, A. C.; Schofield, A.; Weitz, D. A. *Science* **2000**, *287*, 627.
- (35) Zhang, H.; Srolovitz, D. J.; Warren, J.; Douglas, J. F. *Phys. Rev. B* **2006**, *74*, 115404.
- (36) Zhang, H.; Srolovitz, D. J.; Douglas, J. F.; Warren, J. *Acta Mater.* **2007**, *55*, 4527.
- (37) Keys, A. S.; Abate, A. R.; Glotzer, S. C.; Durian, D. J. *Nat. Phys.* **2007**, *3*, 260.
- (38) Adam, G.; Gibbs, J. H. *J. Chem. Phys.* **1965**, *43*, 139.
- (39) Douglas, J. F.; Dudowicz, J.; Freed, K. F. *J. Chem. Phys.* **2006**, *125*, 144907.
- (40) Riggleman, R. A.; Douglas, J. F.; De Pablo, J. J. *Phys. Rev. E* **2007**, *76*, 011504.
- (41) Bai, X. M.; Li, M. *Phys. Rev. B* **2008**, *77*, 134109.
- (42) Van Workum, K.; Douglas, J. F. *Phys. Rev. E* **2005**, *71*, 031502.
- (43) Van Workum, K.; Douglas, J. F. *Phys. Rev. E* **2006**, *73*, 031502.
- (44) Stukalin, E. B.; Douglas, J. F.; Freed, K. F. *J. Chem. Phys.* **2008**, *129*, 094901.
- (45) Sciortino, F.; Bianchi, E.; Douglas, J. F.; Tartaglia, P. *J. Chem. Phys.* **2007**, *126*, 194903.
- (46) Sciortino, F.; De Michele, C.; Douglas, J. F. *J. Phys.: Condens. Matter* **2008**, *20*, 155101.
- (47) Lin, I.; Juan, W. T.; Chiang, C. H.; Chu, J. H. *Science* **1996**, *272*, 1626.
- (48) Alder, B. J.; Hoover, W. G.; Wainwright, T. E. *Phys. Rev. Lett.* **1963**, *11*, 241.
- (49) Alder, B. J.; Ceperley, D. M.; Pollock, E. L. *Int. J. Quantum Chem.* **1982**, *16*, 49.
- (50) Naidoo, K. J.; Schnitker, J.; Weeks, J. D. *Mol. Phys.* **1993**, *80*, 1.
- (51) Murray, C. A.; Wenk, R. A. *Phys. Rev. Lett.* **1989**, *62*, 1643.
- (52) Murray, C. A.; Van Winkle, D. H. *Phys. Rev. Lett.* **1987**, *58*, 1200.
- (53) Tang, Y.; Armstrong, A. J.; Mockler, R. C.; Osullivan, W. J. *Phys. Rev. Lett.* **1989**, *62*, 2401.
- (54) Marcus, A. H.; Rice, S. A. *Phys. Rev. E* **1997**, *55*, 637.
- (55) Pouliquen, B.; Malzbender, R.; Ryan, P.; Clark, N. A. *Phys. Rev. B* **1990**, *42*, 988.
- (56) Choquard, P.; Clerouin, J. *Phys. Rev. Lett.* **1983**, *50*, 2086.
- (57) Thomas, H. M.; Morfill, G. E. *Nature* **1996**, *379*, 806.
- (58) Frenken, J. W. M.; Maree, P. M. J.; Vanderveen, J. F. *Phys. Rev. B* **1986**, *34*, 7506.
- (59) Wang, L.; Peng, C. X.; Wang, Y. Q.; Zhang, Y. N. *Phys. Lett. A* **2006**, *350*, 69.
- (60) McKenna, G. B.; Leterrier, Y.; Schultheisz, C. R. *Polym. Eng. Sci.* **1995**, *35*, 403.
- (61) Starr, F. W.; Douglas, J. F. *Phys. Rev. Lett.* **2011**, *106*, 115702.
- (62) Adams, G.; Gibbs, J. H. *J. Chem. Phys.* **1965**, *43*, 139.
- (63) Lee, H. -N.; Paeng, K.; Swallen, S. F.; Ediger, M. D. *Science* **2009**, *323*, 231.
- (64) Lee, H. -N.; Riggleman, R. A.; de Pablo, J.; Ediger, M. D. *Macromolecules* **2009**, *42*, 4328.
- (65) Van Workum, K.; Douglas, J. F. *Phys. Rev. E* **2005**, *71*, 031502.
- (66) Sciortino, F.; Bianchi, E.; Douglas, J. F.; Tartaglia, P. *J. Chem. Phys.* **2011**, *134*, 124902.
- (67) Sciortino, F.; De Michele, C.; Douglas, J. F. *J. Phys.: Condens. Matter* **2008**, *20*, 155101.
- (68) Angelini, T. E.; Hannezo, E.; Trepat, X.; Marquez, M.; Fredberg, J. J.; Weitz, D. A. *Proc. Natl. Acad. Sci. U.S.A.* **2011**, *108*, 4714.
- (69) Zhou, Y.; Vitkup, D.; Karplus, M. *J. Mol. Biol.* **1999**, *29*, 1371.
- (70) Koparde, V. N.; Cummings, P. T. *ACS Nano* **2008**, *2*, 1620.
- (71) Koparde, V. N.; Cummings, P. T. *J. Phys. Chem. B* **2005**, *109*, 24280.
- (72) Giovambattista, N.; Buldyrev, S. V.; Starr, F. W.; Stanley, H. E. *Phys. Rev. Lett.* **2003**, *90*, 085506.
- (73) Millett, P. C.; Selvam, R. P.; Saxena, A. *Acta Mater.* **2006**, *54*, 297.
- (74) Starr, F. W.; Sastry, S.; Douglas, J. F.; Glotzer, S. C. *Phys. Rev. Lett.* **2002**, *89*, 125501.
- (75) Larini, L.; Ottociani, A.; De Michele, C.; Leporini, D. *Nat. Phys.* **2008**, *4*, 42.
- (76) Dudowicz, J.; Freed, K. F.; Douglas, J. F. *Adv. Chem. Phys.* **2007**, *137*, 125.